

SCIENTIFIC REPORTS



OPEN

A chalcone derivative reactivates latent HIV-1 transcription through activating P-TEFb and promoting Tat-SEC interaction on viral promoter

Jun Wu¹, Ming-tao Ao¹, Rui Shao¹, Hui-ru Wang¹, Diao Yu¹, Mei-juan Fang¹, Xiang Gao¹, Zhen Wu¹, Qiang Zhou² & Yu-hua Xue¹

The principal barrier to the eradication of HIV/AIDS is the existence of latent viral reservoirs. One strategy to overcome this barrier is to use latency-reversing agents (LRAs) to reactivate the latent proviruses, which can then be eliminated by effective anti-retroviral therapy. Although a number of LRAs have been found to reactivate latent HIV, they have not been used clinically due to high toxicity and poor efficacy. In this study, we report the identification of a chalcone analogue called Amt-87 that can significantly reactivate the transcription of latent HIV proviruses and act synergistically with known LRAs such as prostratin and JQ1 to reverse latency. Amt-87 works by activating the human transcriptional elongation factor P-TEFb, a CDK9-cyclin T1 heterodimer that is part of the super elongation complex (SEC) used by the viral encoded Tat protein to activate HIV transcription. Amt-87 does so by promoting the phosphorylation of CDK9 at the T-loop, liberating P-TEFb from the inactive 7SK snRNP, and inducing the formation of the Tat-SEC complex at the viral promoter. Together, our data reveal chalcones as a promising category of compounds that should be further explored to identify effective LRAs for targeted reversal of HIV latency.

The latent HIV reservoir, which contains integrated but transcriptionally silent proviruses, is the principal obstacle to the eradication of HIV/AIDS^{1,2}. Effective curative strategies aiming at eliminating the reservoir are being developed³⁻⁹. One such strategy, nicknamed “shock and kill”, proposes to reactivate the latent HIV proviruses with latency-reversing agents (LRAs) in the initial “shock” phase. This is followed in the “kill” phase by the use of highly active anti-retroviral therapy (HAART) to prevent new infections and at the same time by making the reactivated cells sensitive to the host immune system and viral cytopathogenicity¹⁰⁻¹². The implementation of the “shock and kill” strategy has so far been hindered by the lack of clinically effective LRAs. All the available LRAs such as the HDAC inhibitor SAHA, PKC agonist prostratin and BET bromodomain inhibitor JQ1 are either highly toxic or display poor clinical outcomes¹³⁻¹⁵. Thus, high efficacious and specific drugs for reactivating latent HIV are urgently needed.

The reactivation of latent proviral transcription requires the HIV-encoded trans-activator protein Tat, which stimulates the elongation stage of RNA polymerase (Pol) II transcription to produce the full-length viral transcripts¹⁴. Tat acts by recruiting the host super elongation complex (SEC) containing CDK9, cyclin (Cyc)T1, AFF1 or AFF4, ELL1 or ELL2, and AF9 or ENL to the viral TAR RNA element, which is a stem-loop structure formed at the 5' end of the nascent HIV transcript^{16,17}. Once recruited, the SEC components CDK9 and CycT1, which forms a heterodimer referred to as P-TEFb, phosphorylates the C-terminal domain of the largest subunit of Pol II and a pair of negative elongation factors DSIF and NELF, leading to the release of Pol II from promoter-proximal

¹School of Pharmaceutical Sciences and Fujian Provincial Key Laboratory of Innovative Drug Target Research, Xiamen University, Xiamen, Fujian, 361005, China. ²Department of Molecular and Cell Biology, University of California, Berkeley, Berkeley, CA94720, USA. Jun Wu and Ming-tao Ao contributed equally to this work. Correspondence and requests for materials should be addressed to Z.W. (email: wuzhen@xmu.edu.cn) or Q.Z. (email: qzhou@berkeley.edu) or Y.-h.X. (email: xueyuhua@xmu.edu.cn)

pausing. On the other hand, the ELL1/2 subunit of the SEC can also directly stimulate the processivity of Pol II by suppressing transient pausing. Thus, working from a single Tat-SEC complex, P-TEFb and ELL1/2 can synergistically activate Pol II elongation along the proviral DNA to reverse HIV latency^{18–21}.

In latently infected T cells, the vast majority of P-TEFb is sequestered in a catalytically inactive complex called the 7SK snRNP⁴. In addition to P-TEFb, this 7SK snRNP also contains the 7SK snRNA that acts as a molecular scaffold to hold the complex together and the HEXIM protein, which functions as an inhibitor of CDK9^{17, 22–25}. Within the 7SK snRNP, the-La related protein LARP7 and the 7SK snRNA capping enzyme MePCE are also constitutive components, which stabilize the 7SK snRNA and may also be involved in regulating the release of P-TEFb^{26–29}. The sequestration of P-TEFb in 7SK snRNP keeps the overall P-TEFb/SEC activity in a cell at a very low level and has been proposed as a key factor contributing to HIV latency²⁶.

Chalcones, also known as chalconoids, are aromatic ketones that contain two phenyl rings and often emerge as intermediates in the synthesis of many biological compounds. They have been shown to possess an array of biological activities including anti-inflammatory, antioxidant, antitumor and antibacterial activities and can also inhibit angiogenesis *in vivo* and *in vitro*^{30–35}. Chalcone analogues have attracted a great deal of interest due to their synthetic and biological importance in medicinal chemistry³⁶. Recently, in a screen for LRAs that can reverse HIV latency, we have come upon a series of 2'-hydroxy-5-adamantyl-chalcones that display such an activity. One of them, called Amt-87, dose-dependently activates HIV transcription while displaying only mild cytotoxicity. It can also synergize with traditional LRAs such as prostratin and JQ1 to reactivate latent proviruses. Mechanistically, Amt-87 is shown to increase the phosphorylation of the CDK9 T-loop at position Thr186, dissociate P-TEFb from 7SK snRNP, and promote the assembly of the Tat-SEC complex on the HIV-1 LTR. Together, these data have revealed chalcones as a promising category of compounds that should be further explored to identify effective LRAs for targeted reversal of HIV latency.

Results

Identification of Amt-87 as a HIV latency-reversal agent (LRA). To identify LRAs that can effectively reverse HIV latency, a systematic screen for compounds or natural products present in a library established in the School of Pharmaceutical Sciences at Xiamen University was conducted. This library contained chemically synthesized compounds as well as purified native products derived from traditional Chinese medicinal herbs, marine microbial secondary metabolites, and symbiotic bacteria secondary metabolites³⁷. For detection of latency reversal, we employed the Jurkat T cell line-based J-Lat A2 system, which contains an integrated HIV-1 5'-LTR-Tat-Flag-iRES-EGFP-3'-LTR expression cassette³⁸. This cassette is normally silent but produces the enhanced green fluorescent protein (GFP) upon activation, which can be detected by flow cytometry (FACS).

Among a family of structurally related chalcone derivatives, we found that significant induction of GFP expression in J-Lat A2 cells, i.e. reversal of HIV-1 latency, was caused by members **1a**, **1d**, **1h**, and **1i** (Table 1). The general method for the synthesis of 2'-hydroxy-chalcone amide derivatives (**1a–1p**) is outlined in Supplemental Information (Supplementary Fig. S1). Unfortunately, all four also markedly reduced cell viability (Table 2). To decrease the toxicity of these compounds and at the same time preserve their latency-reversing potential, we generated another two series of chalcone derivatives with functional group adamant (Ad) at the C5-position of the benzene ring system (**3a–3d** and **4a–4d**, see Table 1). Among these new derivatives, compound **3d** [(E)-3-(5-(adamantan-1-yl)-2,4-bis(methoxymethoxy) phenyl)-1-(2-hydroxy-5-methylphenyl)prop-2-en-1-one], called Amt-87 henceforth, effectively induced GFP production in J-Lat A2 cells at 50 and 100 µg/mL, while displaying significantly diminished cell toxicity at these concentrations compared to compounds in the other series (Table 2).

The chemical structure of Amt-87 is shown in Fig. 1A and its purity was confirmed by High-Performance Liquid Chromatography with Diode-Array Detection (HPLC-DAD) performed at 254 nm (up) and 280 nm (down) in Fig. 1B, as well as the examination by ¹H-NMR (left) and ¹³C-NMR (right) in Fig. 1C. The general chemistry of the synthesis of Amt-87 is outlined in Supplemental Information (Supplementary Fig. S2). To further determine whether Amt-87 may affect cell growth, we used the Promega CellTiter-Glo[®] Luminescent Cell Viability Assay kit to measure the viability of both J-Lat A2 and HeLa cells that were treated with Amt-87 at concentrations of 50, 100 and 200 µg/mL for 24 hours. As indicated in Fig. 1D, these concentrations had no or only a very minor effect on the viability of HeLa cells when compared with the empty vehicle DMSO. For J-Lat A2, although these cells were more sensitive to Amt-87, treatment with 50 µg/ml of the drug, which was used in most latency-reversal experiments described below, had a relatively mild effect on cell viability.

Based on the above results showing that among the entire collection of chalcone derivatives, Amt-87 displayed the most optimal properties in terms of its efficient latency-reversing activity and relatively mild cytotoxicity, it was thus selected for further mechanistic study as outlined below.

Amt-87 reactivates latent HIV at the transcriptional level. When J-Lat A2 cells were treated with different amounts of Amt-87 and for various time periods, the percentage of GFP-positive cells increased in a dose- and time-dependent manner (Fig. 2A,B). In addition, the treatment also significantly augmented the mean fluorescence intensity (MFI) of the GFP-positive cells (Supplementary Fig. S3). To confirm that the enhanced GFP signal detected by FACS was due to the increased production of GFP mRNA, quantitative RT-PCR (qRT-PCR) with primers that hybridize to a distal portion of the GFP gene was performed. The result showed that Amt-87 indeed reactivated the HIV provirus through stimulating the LTR-driven mRNA production (Fig. 2C), suggesting that the activation occurred at the transcriptional level.

The 2D10 cell line is another Jurkat-based post-integrative latency model that harbors almost the complete HIV genome except for the *nef* gene that is replaced by the GFP-coding sequence³⁹. Importantly, the stimulatory effect of Amt-87 to reactivate latent HIV was also confirmed in this system (Fig. 2D). Finally, to ensure that the Amt-87-induced HIV transactivation was dependent on the viral 5'-LTR but not any other unrelated viral or non-viral sequences in the integrated expression cassette, we tested the effect of Amt-87 on expression of an

Compound	Structures		% GFP(+) cells (50 µg/mL)	Compound	Structures		% GFP(+) cells (50 µg/mL)
	R'	R			R'	R	
DMSO			0.7 ± 0.1	1o	2'-OH-4'-CH ₃	3-CONHCH ₂ CH ₂ -3'-Thi	3.1 ± 1.3
Prostratin (2.5 µm)			65.3 ± 5.4	1p	2'-OH-4'-CH ₃	3-CONHCH ₂ CH ₂ Ph	1.8 ± 0.3
1a	2'-OH-5'-CH ₃	4-CONHCH ₂ CH ₂ -3'-Thi	10.3 ± 2.0	2a	2'-OH	2-OH	2.0 ± 0.2
1b	2'-OH-5'-CH ₃	4-CONHPh	4.0 ± 1.5	2b	2'-OH	4-OH	1.2 ± 0.1
1c	2'-OH-5'-CH ₃	4-CONHCH ₂ Ph	—	2c	2'4'-OH	4-OH	1.3 ± 0.2
1d	2'-OH-5'-CH ₃	4-CONH(CH ₂) ₂ Ph	14.3 ± 3.3	2d	2'-OH-5'-CH ₃	4-OH	0.7 ± 0.2
1e	2'-OH-5'-CH ₃	4-CONH(CH ₂) ₃ Ph	—	2e	4'-OH	2-OH-6-OCH ₃ -3-prenyl	1.0 ± 0.2
1f	2'-OH-5'-CH ₃	4-CONH(CH ₂) ₄ Ph	4.2 ± 1.1	3a	2'-OH	4-MOM-5-Ad	—
1g	2'-OH-5'-CH ₃	4-CONHCH ₂ -1-Nap	2.6 ± 1.0	3b	2'-OH-5'-Cl	4-MOM-5-Ad	—
1h	2'-OH-5'-CH ₃	4-CONHPh-2'-OCH ₃	20.7 ± 3.8	3c	2'-OH-5'-CH ₃	4-MOM-5-Ad	3.9 ± 1.0
1i	2'-OH-5'-CH ₃	4-CONHC(CH ₃) ₃	—	3d (Amt-87)	2'-OH-5'-CH ₃	2,4-diMOM-5-Ad	4.9 ± 1.6
1j	2'-OH-5'-CH ₃	4-CONH-cyclo-C ₄ H ₇	—	3e	5'-CH ₃	2,4-diMOM-5-Ad	—
1k	2'-OH-5'-CH ₃	4-CONH(CH ₂) ₅ CH ₃	4.1 ± 1.2	4a	2'-OH	4-OH-5-Ad	—
1l	2'-OH-5'-CH ₃	4-CONH(CH ₂) ₇ CH ₃	6.5 ± 1.4	4b	2'-OH-5'-Cl	4-OH-5-Ad	—
1m	2'-OH-5'-CH ₃	4-CONH-cyclo-C ₈ H ₁₅	—	4c	2'-OH-5'-CH ₃	4-OH-5-Ad	3.5 ± 0.7
1n	2'-OH-5'-CH ₃	4-CONH-1-Ad	1.5 ± 0.2	4d	2'-OH-5'-CH ₃	2,4-OH-5-Ad	—

Table 1. Reactivation of latent HIV-1 gene expression by the indicated chalconoids in J-Lat A2 cells. J-Lat A2 cells were treated for 24 hr with the empty vehicle DMSO, prostratin (2.5 µM) or the various chalconoids (50 µg/mL) of the indicated structures. Levels of HIV latency reversal were evaluated by FACS analysis to measure the percentage of cells that displayed the HIV LTR-driven GFP production. Data are presented as mean ± SD from at least three independent experiments performed in triplicates.

Compound	R''	% GFP(+) cells (µg/mL)			% Cell viability (µg/mL)		
		25	50	100	25	50	100
1a	4-CONHCH ₂ CH ₂ -3'-Thi	6.6 ± 0.7	9.2 ± 2.3	8.3 ± 1.6	67.1 ± 6.8	54.3 ± 5.4	41.8 ± 4.2
1b	4-CONHPh	3.1 ± 0.6	3.6 ± 1.2	3.0 ± 0.8	31.5 ± 4.4	15.7 ± 3.1	7.9 ± 2.2
1d	4-CONH(CH ₂) ₂ Ph	13.7 ± 1.6	15.1 ± 2.4	15.7 ± 2.1	36.9 ± 3.9	35.0 ± 2.6	28.9 ± 3.7
1f	4-CONH(CH ₂) ₄ Ph	2.5 ± 0.7	4.0 ± 1.3	7.2 ± 1.3	68.8 ± 3.1	65.2 ± 4.2	58.5 ± 4.5
1g	4-CONHCH ₂ -1-Nap	10.3 ± 2.0	2.8 ± 1.0	1.8 ± 0.8	37.2 ± 6.2	27.9 ± 3.2	9.5 ± 1.5
1h	4-CONH-Ph-2'-OCH ₃	18.3 ± 1.3	22.5 ± 3.4	33.7 ± 3.6	49.3 ± 5.3	42.7 ± 4.0	12.3 ± 2.1
1k	4-CONH(CH ₂) ₅ CH ₃	3.7 ± 1.2	3.9 ± 1.1	3.1 ± 1.0	67.6 ± 3.2	63.2 ± 4.2	53.3 ± 3.6
1l	4-CONH(CH ₂) ₇ CH ₃	7.1 ± 1.7	8.4 ± 1.4	6.7 ± 1.5	24.7 ± 2.3	24.3 ± 2.7	19.5 ± 2.1
1o	3-CONHCH ₂ CH ₂ -3'-Thi	0.8 ± 0.1	3.8 ± 1.2	0.7 ± 0.1	36.4 ± 2.3	34.8 ± 2.7	37.3 ± 3.4
1p	3-CONH(CH ₂) ₂ Ph	0.9 ± 0.1	2.1 ± 0.2	0.6 ± 0.1	42.0 ± 4.4	31.1 ± 2.0	31.2 ± 3.2
3c	4-MOM-5-Ad	0.7 ± 0.1	4.3 ± 1.1	13.3 ± 1.8	95.3 ± 3.5	92.5 ± 4.3	68.4 ± 4.2
3d (Amt-87)	2,4-diMOM-5-Ad	0.8 ± 0.1	5.9 ± 1.5	38.0 ± 4.2	96.3 ± 3.8	91.5 ± 3.4	72.9 ± 4.9
4c	4-OH-5-Ad	0.7 ± 0.1	3.8 ± 0.7	11.2 ± 2.0	86.4 ± 3.7	68.9 ± 6.3	45.4 ± 5.1

Table 2. Viability and GFP production in J-Lat A2 cells treated with the indicated chalconoids. J-Lat A2 cells were treated with the indicated compounds at 25, 50 and 100 µg/mL concentrations for 24 hr and the percentage of GFP(+) cells and cell viability were evaluated by FACS and Cell viability analysis, respectively. Data are presented as mean ± SD from at least three independent experiments that were performed in triplicates.

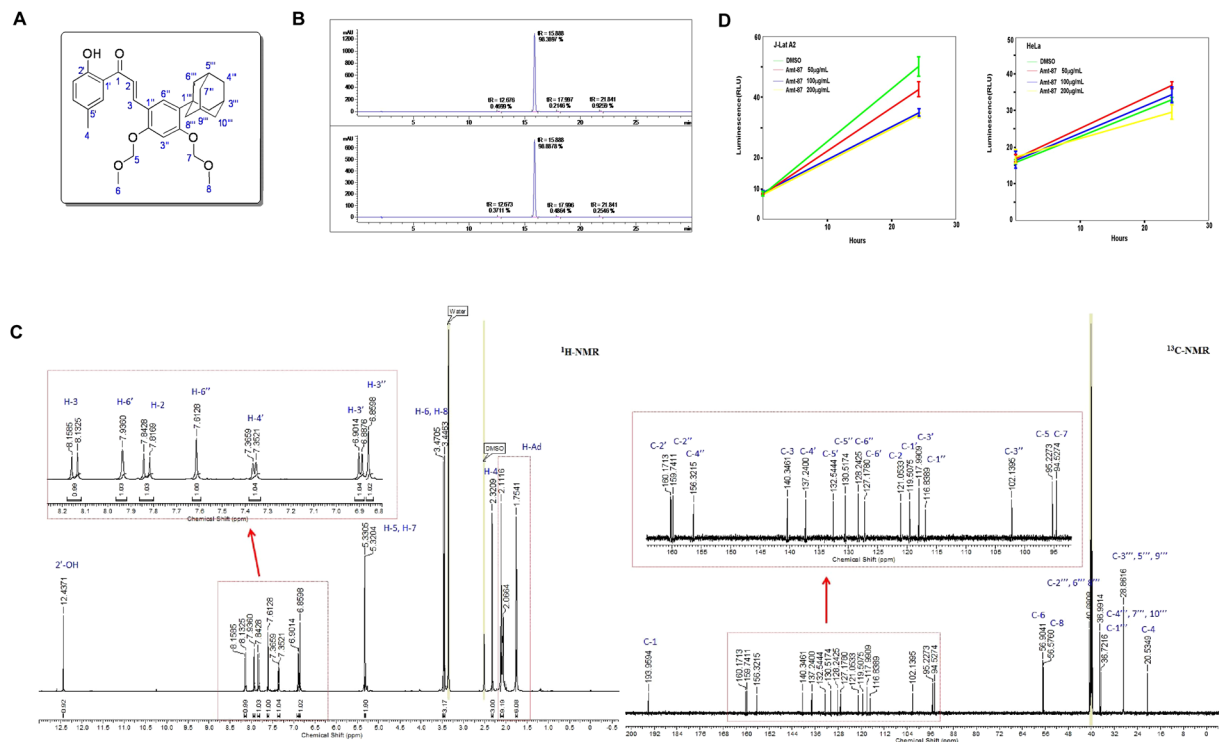


Figure 1. Purity analysis, structure confirmation and effect on cell viability of compound Amt-87. **(A)** The chemical structure of Amt-87 showing atom numbering. **(B)** HPLC-DAD analysis of Amt-87 performed at 254 nm (up) and 280 nm (down) is presented. The purity of Amt-87 is estimated to be above 98%. **(C)** The ^1H -NMR (left) and ^{13}C -NMR (right) spectra of Amt-87 are shown. The peaks in the spectra are identified and assigned to the structure. **(D)** The impact of Amt-87 on viability of J-Lat A2 and HeLa cells was measured at the indicated time points after the commencement of treatment by using the Promega CellTiter-Glo[®] Luminescent Cell Viability Assay kit. The error bars represent mean \pm SD from three independent experiments.

integrated luciferase reporter gene that is driven solely by the HIV-1 5'-LTR in a pair of HeLa-based isogenic cells lines, NH1 and NH2, both of which contain an integrated HIV-1 5'-LTR-luciferase reporter gene but only the latter stably expresses HIV-1 Tat^{40,41}. When these cells were treated with different amounts of Amt-87 and for various time periods as indicated in Fig. 2E–H, Amt-87 displayed a stimulatory effect on both Tat-independent and -dependent HIV-1 transcription in a dose- and time-dependent manner.

Amt-87 synergizes with conventional LRAs prostratin and JQ1 to reactivate latent HIV.

Previous studies have identified several classes of chemical compounds that can reactivate latent HIV. For example, prostratin is the prototype of protein kinase C (PKC) agonist that acts through and NF- κ B pathway to promote the recruitment of RNA Pol II to the HIV-1 LTR⁴². On the other hand, JQ1, a BET bromodomain inhibitor, induces the reversal of HIV latency through antagonizing the inhibitory action of Brd4 on Tat-dependent activation of HIV transcriptional elongation⁴³. To investigate how Amt-87 might work together with these two known conventional LRAs, J-Lat A2 cells were treated with Amt-87 alone or in combination with prostratin (Fig. 3A) or JQ1 (Fig. 3B). The data indicate that the combined treatments produced a much greater percentage of GFP(+) cells than the simple sum of the effects produced by either compound alone. Notably, the synergism displayed by Amt-87 together with prostratin or JQ1 was also recapitulated in NH1 cells containing the integrated HIV-1 LTR-driven luciferase reporter gene (Fig. 3C,D).

CDK9 kinase activity is required for Amt-87 to reverse HIV latency. P-TEFb, which is composed of CDK9 and CycT1, plays a key role in HIV transcriptional activation, and its sequestration in the inactive 7SK snRNP has been proposed to contribute to viral latency¹⁵. To determine whether the kinase activity of CDK9 is required for Amt-87 to induce latency reversal, J-LatA2 cells were pre-treated with the CDK9 inhibitor flavopiridol⁴⁴ or the more selective CDK9 inhibitor iCDK9⁴⁵ before the incubation with Amt-87. As shown in Fig. 4A,B, these two drugs completely blocked the reactivation of HIV latency induced by Amt-87.

The dependence on CDK9 kinase activity for Amt-87's stimulatory effect was also observed in NH1 cells, where the pre-treatment with not only flavopiridol (Fig. 4C) but also iCDK9 (Fig. 4D) markedly suppressed the ability of Amt-87 to activate the LTR-driven luciferase expression. Finally, similar to these two small molecule inhibitors of CDK9, D167N, a dominant negative form of CDK9⁴⁶, was also able to prevent Amt-87 from activating the HIV-1 LTR once overexpressed in NH1 cells (Fig. 4E). Taken together, these data indicate that the reversal of HIV latency by Amt-87 depended on CDK9's kinase activity.

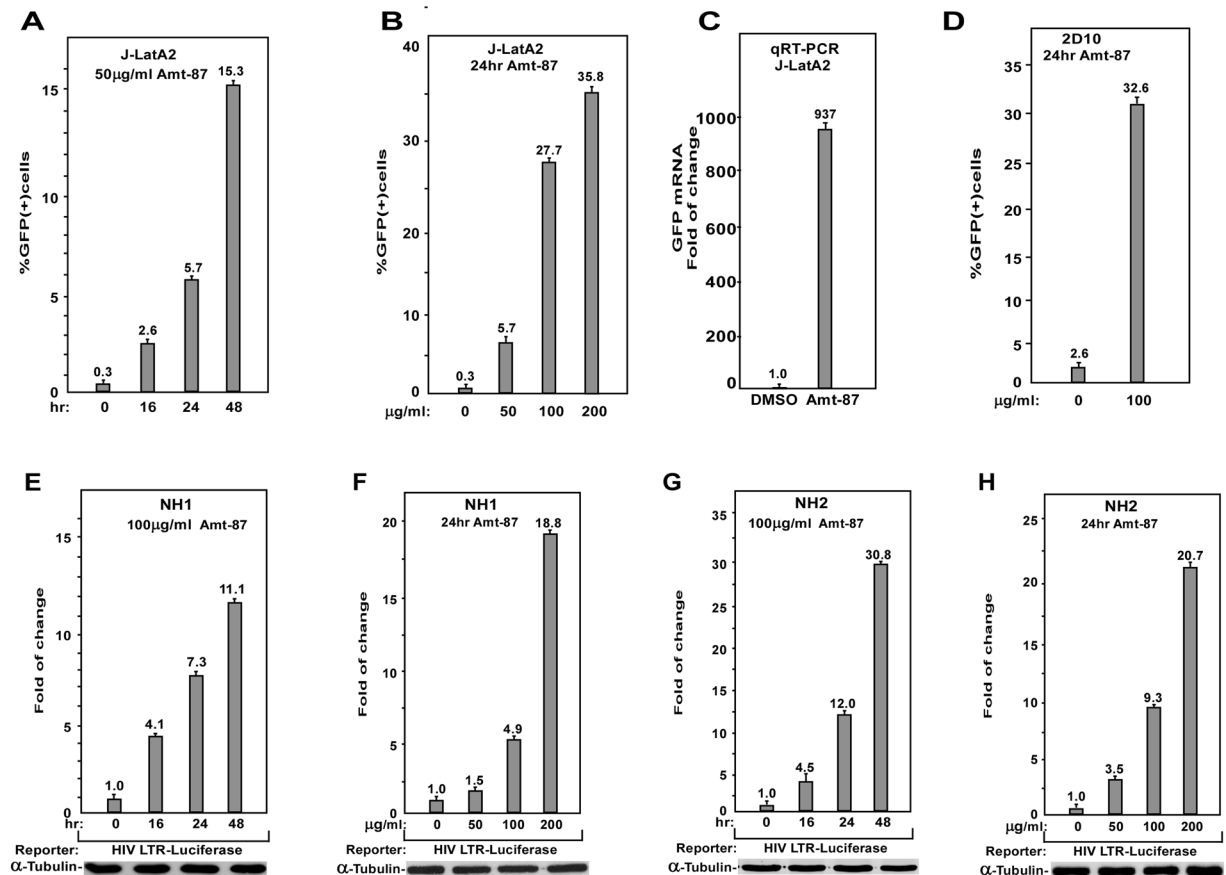


Figure 2. Amt-87 promotes reversal of HIV latency in a time- and dose-dependent manner. (A,B) J-LatA2 cells were treated with 50 µg/ml of Amt-87 for the indicated time periods (A) or the indicated concentrations of the drug for 24 hr (B). The percentages of cells expressing GFP were measured by FACS and plotted. (C) J-LatA2 cells were treated with DMSO or 200 µg/ml Amt-87 for 24 hr. The GFP mRNA levels were measured by qRT-PCR and normalized to those of GAPDH and plotted, with the value in DMSO-treated cells adjusted to 1. (D) Jurkat 2D10 cells were treated with 100 µg/ml of Amt-87 or DMSO for 24 hr and the expression of GFP was analyzed by FACS and plotted. (E,F) The HeLa-based NH1 cells containing an integrated HIV LTR-luciferase reporter gene were treated with 100 µg/ml of Amt-87 for the indicated time periods (E) or 24 hr with the indicated concentrations of the drug (F). (G,H) The NH2 cells expressing Tat were treated with 100 µg/ml of Amt-87 for the indicated time periods (G) or 24 hr with in indicated concentrations of the drug (H). Whole cell extracts were prepared and examined for the luciferase activities. The error bars in all panels represent mean \pm SD based on at least three independent experiments.

Amt-87 promotes CDK9 T-loop phosphorylation. Given the above demonstrations that the stimulatory effect of Amt-87 depends on the active P-TEFb and the fact that the activation of P-TEFb during transcription elongation requires the phosphorylation of CDK9 on Thr186 at the T-loop^{47, 48}, we next examined the phosphorylation status of Thr186 in NH1 and J-LatA2 cells after the treatment with Amt-87. Western analysis employing the phospho-Thr186 (pThr186)-specific antibody⁴⁷, revealed that the level of phosphorylation on the CDK9 T-loop significantly increased upon the treatment in both cell lines (Fig. 5A).

In order to release Pol II from promoter-proximal pausing, active P-TEFb is known to phosphorylate the Pol II CTD on Ser2 and the Spt5 subunit of DSIF on Thr775⁴⁵. We next performed Western blotting analysis using phospho-specific antibodies to examine the effect of Amt-87 on the phosphorylation status at these two positions. As shown in Fig. 5B, Amt-87 increased the levels of both pSer2 and pThr775, and this increase was abolished when CDK9 activity was inhibited by flavopiridol. Collectively, these data demonstrate that Amt-87 reactivated HIV latency through enhancing the phosphorylation of the CDK9 T-loop at Thr186, which turned on P-TEFb's kinase activity to phosphorylate Pol II CTD on Ser2 and DSIF Spt5 on Thr775 to activate HIV transcriptional elongation.

Amt-87 induces P-TEFb dissociation from 7SK snRNP and promotes Tat-SEC formation on HIV-1 LTR. In latently infected cells, most of the cellular P-TEFb are sequestered in the inactive 7SK snRNP, and the release of P-TEFb from this complex is essential for latency reactivation⁴. Since Amt-87 has been shown above to activate P-TEFb by causing Thr186 phosphorylation on CDK9, we asked whether this drug is capable of inducing P-TEFb's dissociation from 7SK snRNP. To answer this question, anti-Flag immunoprecipitation was

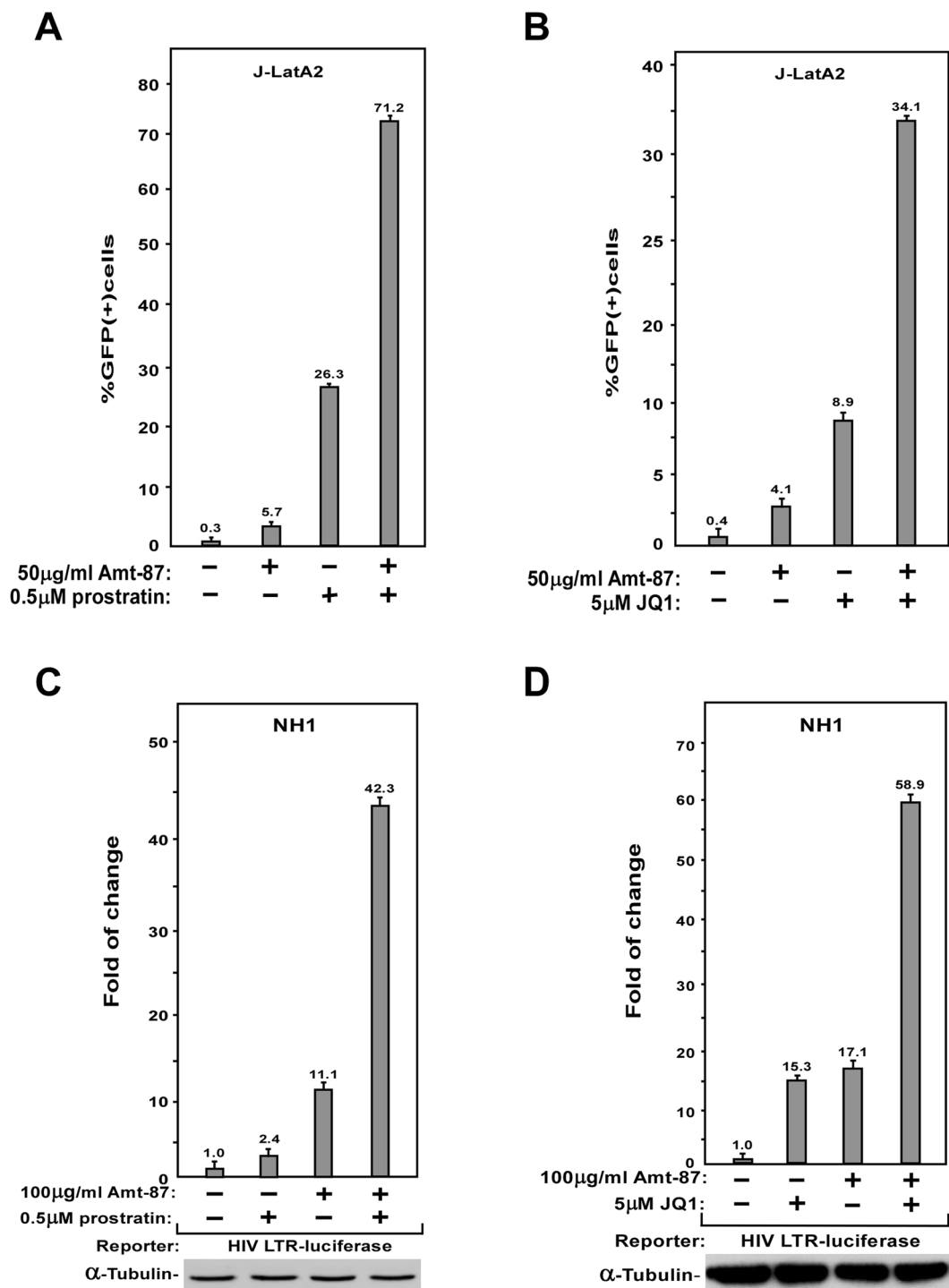


Figure 3. Amt-87 synergizes with prostratin and JQ1 to reverse HIV latency and reactivate viral transcription. (A,B) J-LatA2 cells were pretreated with prostratin (A) or JQ1 (B) for 2 hr, incubated with the indicated concentrations of Amt-87 for 24 hr, and then analyzed by FACS to determine the percentages of GFP(+) cells. (C,D) NH1 cells were pretreated with prostratin (A) or JQ1 (B) for 2 hr, incubated with the indicated concentrations of Amt-87 for 24 hr, and then analyzed by FACS to determine the percentages of GFP(+) cells. Whole cell extracts (WCE) were examined for luciferase activities. The error bars in all panels represent mean \pm SD from three independent experiments.

performed in the HeLa-based F1C2 cells, which stably express the Flag-tagged CDK9 (CDK9-Flag)⁴¹, to examine the association of CDK9 with two signature 7SK snRNP components HEXIM1 and LARP7, which inhibits the CDK9 kinase activity and binds to the 3' end of 7SK snRNA, respectively⁴⁹. Using DMSO as a negative control,

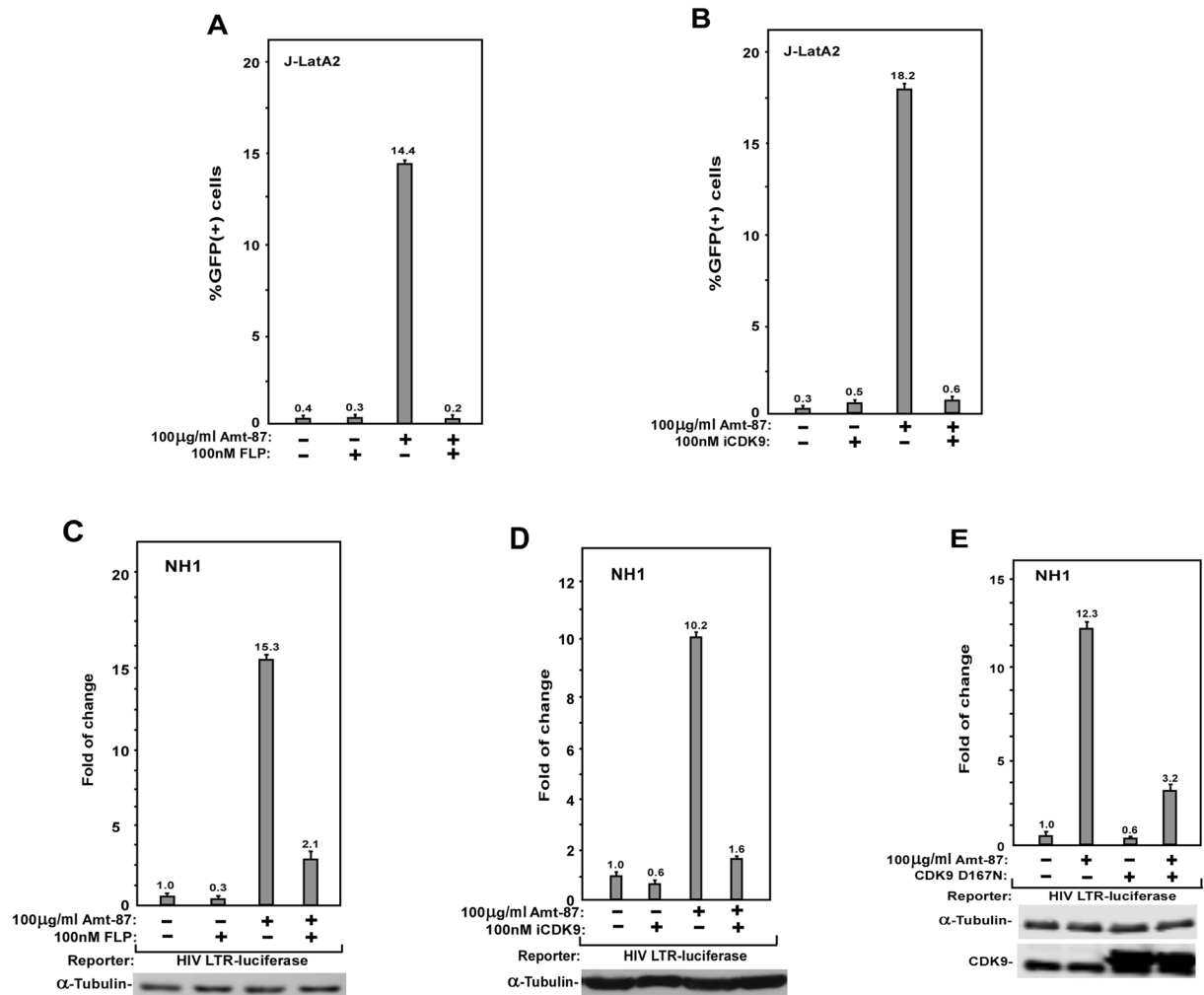


Figure 4. The kinase activity CDK9 is essential for Amt-87 to reactivate latent HIV-1 transcription. (A,B) J-LatA2 cells were pre-treated with flavopiridol (A) or iCDK9 (B) for 2 hr and then treated with Amt-87 for 24 hr at the indicated concentrations. The percentages of GFP(+) cells were determined by FACS and plotted. (C,D) NH1 cells were pre-treated with flavopiridol (C) or iCDK9 (D) and then treated with Amt-87 at the indicated concentrations for 24 hr. Whole cell extracts (WCE) were examined for luciferase activities. (E) NH1 cells were transfected with the plasmid expressing CDK9 mutant D167N and then treated with Amt-87 for 24 hr at the indicated concentration. WCE were examined for luciferase activities. The error bars in all panels represent mean \pm SD from three independent experiments.

we found that Amt-87 markedly reduced the amounts of HEXIM1 and LARP7 bound to the immunoprecipitated CDK9-Flag (Fig. 6A), indicating a disruption of the 7SK snRNP in Amt-87-treated cells.

Given the ability of Amt-87 to directly disrupt 7SK snRNP and activate P-TEFb, we next investigated whether the released P-TEFb can be recruited by HIV-1 Tat into a SEC to form the Tat-SEC complex for activation of HIV transcription and latency reversal. Indeed, anti-Flag immunoprecipitates derived from the HeLa-based NH1 cells expressing Tat-Flag showed increased associations of the signature SEC components AFF4, ELL2, ENL, CDK9 and CycT1 with Tat-Flag upon the exposure to Amt-87 (Fig. 6B), suggesting an enhanced interaction between Tat and the SEC in Amt-87-treated cells.

To determine whether the enhanced Tat-SEC formation promoted by Amt-87 would result in an increased occupancy of the SEC at the HIV-1 promoter region, we performed the ChIP-qPCR analysis to examine the levels of CDK9, AFF4, ELL2 as well as the key 7SK snRNP subunit HEXIM1 at three separate locations along the integrated HIV-1 LTR-luciferase reporter gene. Indeed, compared to DMSO, Amt-87 increased the bindings of SEC components ELL2 and AFF4 as well as CDK9 at and around the HIV-1 promoter region, and decreased the binding of HEXIM1 especially at the HIV-1 promoter (Fig. 6C). These results are consistent with the notion that P-TEFb is transferred from the 7SK snRNP to the SEC in the presence of Amt-87. Taken together, these data support the model that by promoting T-loop phosphorylation in CDK9 and release of P-TEFb from 7SK snRNP, Amt-87 can increase the active pool of P-TEFb in the nucleus for formation of more Tat-SEC at the HIV-1 LTR, which in turn activates HIV-1 transcription and reverses viral latency.

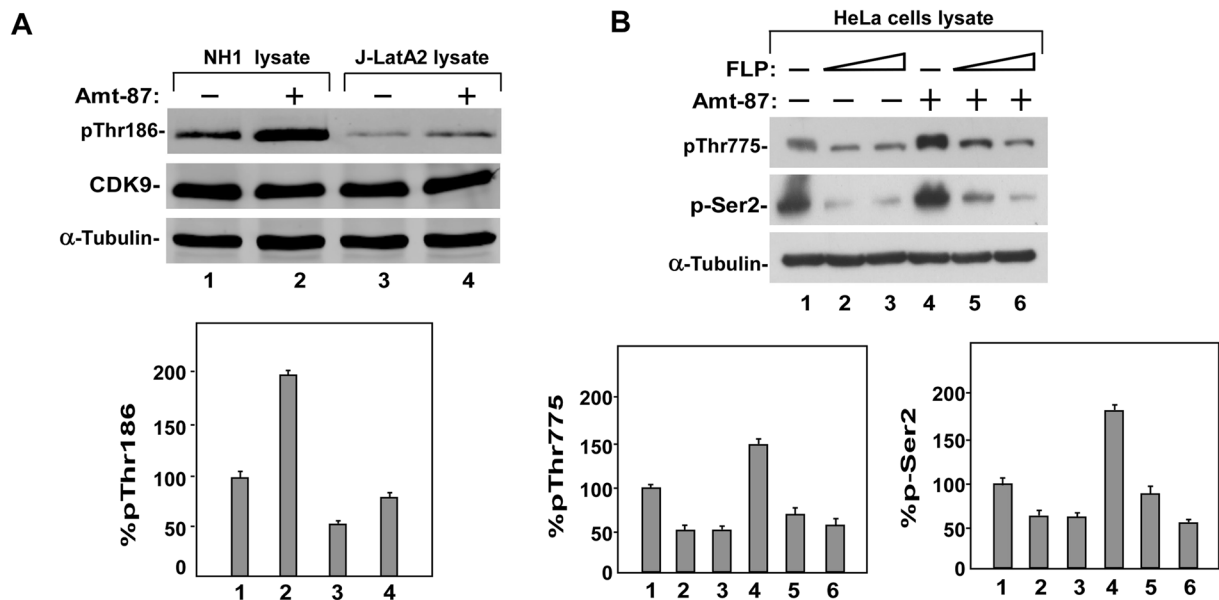


Figure 5. Amt-87 promotes phosphorylation of CDK9 T-loop at Thr186. **(A)** Whole cell lysates derived from NH1 and J-Lat A2 cells, which were treated with (+) or without (-) Amt-87 for 24 hr, were analyzed by Western blotting to detect the levels of total CDK9 and CDK9 phosphorylated on Thr186 (pT186). The levels of pT186 were quantified by densitometry, normalized to those of total CDK9, and shown below the blots, with the level of pT186 in untreated cells (lanes 1 & 3) artificially set at 100%. **(B)** HeLa cells were pre-treated with flavopiridol (FLP) for 2 hr and then treated with Amt-87 for 24 hr. The levels of Pol II CTD phosphorylated on Ser2 (pSer2) and Spt5 phosphorylated on Thr775 (pT775) in whole cell lysates were examined by Western blotting and quantified by densitometry as in A and shown in below the blots.

Discussion

The data presented in the current study are consistent with the notion that Amt-87 promotes the reversal of HIV latency by activating P-TEFb as well as P-TEFb-dependent viral transcription. Surprisingly, Amt-87 is shown to use three different means to activate P-TEFb, namely the induction of phosphorylation on the T-loop of CDK9 at Thr186, the disruption of the inactive 7SK snRNP to release P-TEFb, and lastly the promotion of Tat-SEC interaction on the viral LTR.

The latter two events are likely interconnected and may even have a causative relationship, as the release of P-TEFb from 7SK snRNP is expected to increase the pool of free and active P-TEFb that can be assembled into the SEC and recruited by Tat to the viral promoter region. However, it is unclear whether the Amt-87-induced phosphorylation of CDK9 at Thr186 is mechanistically linked to the disruption of 7SK snRNP. Previously, we and others have shown that even though CDK9 existing in the 7SK snRNP lacks kinase activity, it is nonetheless already phosphorylated at Thr186^{50,51}, an event, by analogy to other structurally determined CDKs⁵², locks the T-loop in an open conformation to allow the access to the catalytic center by the kinase substrate, and thus makes CDK9 poised to become active once liberated from the 7SK snRNP.

What remains to be determined is whether the Amt-87-induced Thr186 phosphorylation contributes to or may even be responsible for the release of P-TEFb from 7SK snRNP. Another aspect of the Amt-87 action that is yet to be investigated concerns how the drug causes the phosphorylation of CDK9 and disruption of 7SK snRNP. Our preliminary data suggest that Amt-87 very likely triggers an unknown signaling pathway leading to these two events, as the incubation of the drug with purified P-TEFb and 7SK snRNP *in vitro* affected neither the T-loop phosphorylation nor 7SK snRNP integrity (Supplementary Figs S4 and S5).

Chalconoids, which exist widely in fruits, vegetables, spices and tea, have interested organic and medicinal chemists for many years³⁰. This is because chalconoids and their derivatives are not only important in the biosynthesis of flavonoids as both precursors and products, they also possess numerous pharmacological activities such as antimicrobial, anti-inflammatory, antiviral, and anticancer effects³⁰. Here, we report a novel function of the chalconoid derivative, Amt-87, in the reversal of HIV latency. Using two different Jurkat cell line-based latency models (J-Lat and 2D10) as well as the HIV-1 LTR-driven luciferase reporter system, we provide evidence that Amt-87 promotes the exit of HIV proviruses from latency by stimulating viral transcription. These observations indicate that chalconoids can be a promising category of compounds that should be further explored to identify effective LRAs that can be used alone or in combination with other drugs to induce efficient reversal of HIV latency.

Materials and Methods

Chemistry. All reagents and chalcones 2a–2e were purchased from commercial sources and were used without further purification unless otherwise indicated. Reactions, which required the use of anhydrous, inert atmosphere techniques, were carried out under an atmosphere of nitrogen. Column chromatography was executed

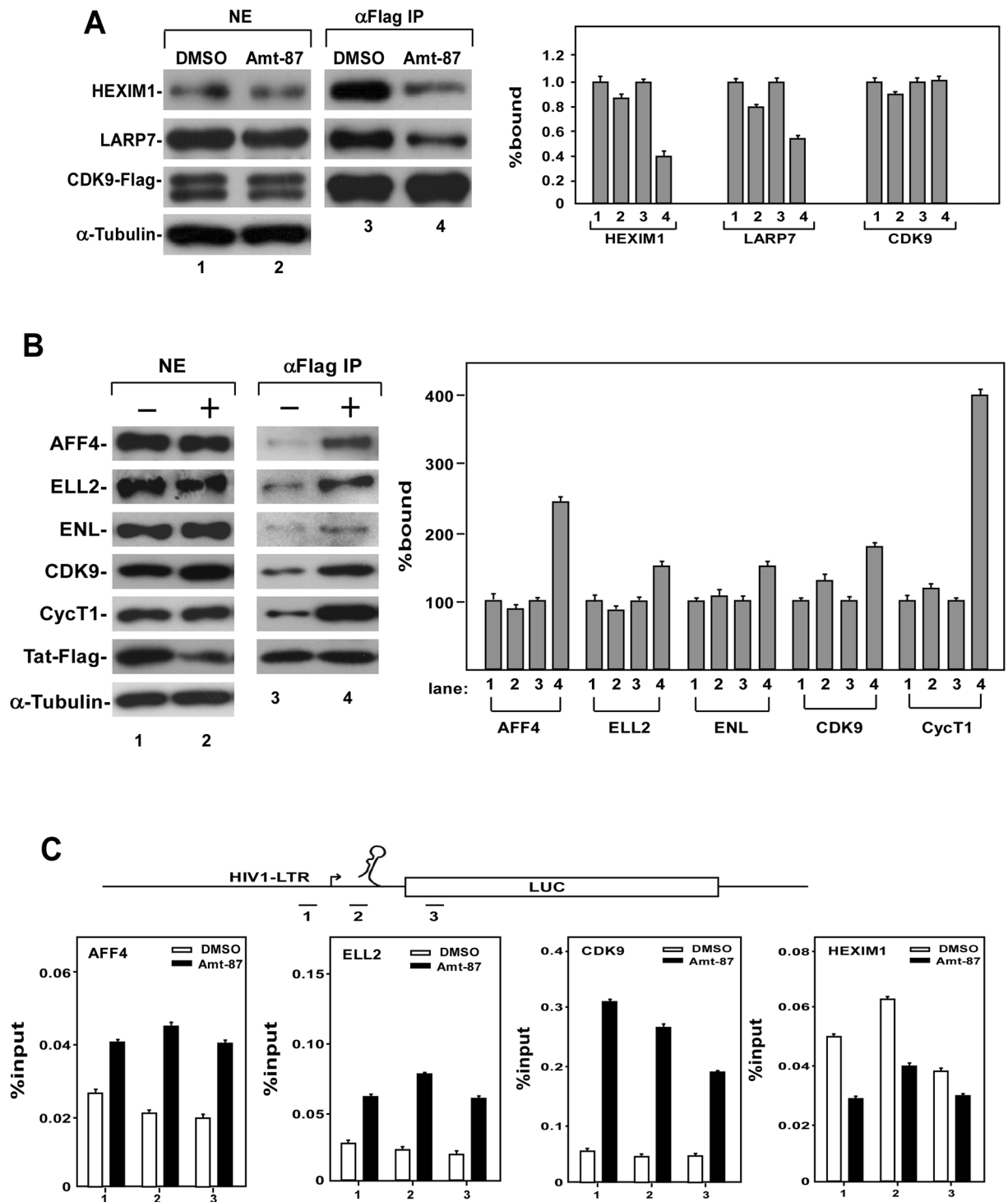


Figure 6. Amt-87 dissociates P-TEFb from 7SK snRNP and promotes Tat-SEC formation at the HIV-1 promoter. (A) The HeLa-based F1C2 cells stably expressing the Flag-tagged CDK9 were treated with Amt-87 or DMSO for 24 hr. Nuclear extracts (NE) and anti-Flag immunoprecipitates (IP) derived from NE were analyzed by Western blotting for the indicated proteins and the results were quantified and shown on the right, with the numbers in lanes 1 and 3 set to 1. (B) NH1 cells transfected with the Tat-Flag-expressing plasmid were treated with Amt-87 (+) or DMSO (–) for 24 hr. NEs and anti-Flag IP derived from NE were analyzed by Western blotting for the indicated proteins. (C) Upon transfection with the plasmid expressing Tat-Flag for 24 hr, NH1 cells were treated with Amt-87 or DMSO for 24 hr and then subjected to ChIP-qPCR analysis to determine the occupancy of the indicated factors at three different locations (1–3) at and around the HIV-1 promoter region (diagramed on top). The ChIP signals were normalized to those of input and plotted, with the error bars indicating mean \pm SD from three independent experiments.

with silica gel (60–120 or 230–400 mesh) using mixtures of ethyl acetate and hexane as eluants. Melting points were measured on a SGW X-4 micro-melting point spectrometer and were uncorrected. ¹H-NMR and ¹³C-NMR spectra were obtained using a Bruker (Bruker Biospin, Zug, Switzerland) AV2 600 Ultrashield spectrometer at 600 and 150 MHz, respectively. Chemical shifts were given in parts per million (ppm) relative to tetramethylsilane (TMS) as an internal standard. Multiplicities were abbreviated as follows: single (s), doublet (d), doublet-doublet (dd), doublet-triplet (dt), triplet (t), triplet-triplet (tt), triplet-doublet (td), quartet (q), quartet-doublet (qd), quint (quin), sext (sxt), multiplet (m), and broad signal (br. s.). High-resolution mass spectral (HRMS) data were acquired using electrospray ionization (ESI) on a Q Exactive LC-MS/MS instrument (Thermo Fisher Scientific Inc., Waltham, MA, USA) with UV detection at 254 nm.

Synthesis. The general method for the synthesis of 2'-hydroxy-chalcone amide derivatives (1a–1p) and 5-adamantyl-chalcones (3a–3e and 4a–4d) are outlined in Supplemental Information, with their structures confirmed by ¹H-NMR, ¹³C-NMR, and HRMS (for details, see Supplemental Information).

HPLC analysis of Amt-87. The purity of Amt-87 was assessed by HPLC with a COSMOSIL C18-MS-II column (250 mm × 4.6 mm i.d., 5 mm). The mobile phase used was acetonitrile (A) and water (B) in a linear gradient mode as follows: A from 80% to 100% and B from 20% to 0% during 0–20 min. The HPLC analysis was performed at a flow rate of 1 mL/min and monitored at 254 nm and 280 nm by the Agilent HPLC system.

Biochemistry. *Reagents, antibodies and cell lines.* Prostratin and JQ1 were purchased from LC Laboratories and Cayman Chemical, respectively. Flavopindol (F3055) was purchased from Sigma. The anti-ENL (A302-267A) and anti-ELL2 (A302-505A) antibodies were purchased from Bethyl Laboratories. The antibodies against α -tubulin (T9026) and Flag (F3165) were obtained from Sigma. Antibodies recognizing CycT1 (SC-8128) and AFF4 (14662-1-AP) were purchased from Santa Cruz Biotechnology and Proteintech, respectively. Rabbit polyclonal antibodies against Brd4, HEXIM1, CDK9, LARP7, pThr186 of CDK9, pSer2 of RNA Pol II and pThr775 of Spt5 have been described previously^{26,47,53}. Rabbit total IgG (I5006) used for ChIP was purchased from Sigma. All the cell lines used in this study were either purchased from American Type Culture Collection (ATCC, Manassas, VA) or described before⁵⁴.

Screening by flow cytometry. The flow cytometry-based screening was performed in J-Lat A2 cells containing the integrated LTR-Tat-IRES-GFP-LTR cassette³⁸ and 2D10 cells harboring the nearly complete HIV-1 genome except for the *nef* gene that is replaced by the GFP-coding sequence³⁹. After incubation with the indicated concentrations of Amt-87 or 0.1% dimethyl sulfoxide (DMSO) as a negative control, cells were harvested and washed twice in 1 × phosphate buffered saline (PBS) and analyzed by flow cytometer on Epics Altra (BECKMAN COULTER) for the percentages of cells expressing GFP.

Luciferase assay. The luciferase assay was conducted in NH1 and NH2, a pair of HeLa-based isogenic cell lines, both of which contain an integrated HIV-1 LTR-luciferase reporter gene but only the latter stably expresses HIV-1 Tat^{40,41}. NH1 and NH2 cells were treated with different amounts of Amt-87 and for various time periods as indicated or DMSO as a negative control. Cell lysates were extracted and subjected to the measurement of luciferase activity using a kit from Promega.

Co-immunoprecipitation (co-IP). The co-immunoprecipitation assay was performed as described¹⁶ with minor modifications. Briefly, to detect the dissociation of 7SK snRNP after drug treatment, nuclear extracts (NEs) were prepared from F1C2 cells, a HeLa-based cell line stably expressing Flag-tagged CDK9⁵³. To detect the drug-induced change of the SEC, NH1 cells were transfected with 20 μ g pRK5M-Tat-Flag. One day later, the cells were treated with 200 μ g/ml Amt-87 or DMSO as a control for 24 hr and then subjected to the preparation of NEs. For anti-Flag IP, NEs were incubated with anti-Flag agarose beads (Sigma) for 2 hr at 4 μ L at a ratio of 10 μ L beads per 100 μ L NEs. After extensive washing, the eluted proteins were analyzed by Western blotting with the indicated antibodies.

Chromatin immunoprecipitation (ChIP) assay. The assay was performed essentially as described⁵⁵ with minor modifications. Briefly, NH1 cells containing a stably integrated HIV-1 LTR-luciferase reporter gene were transfected with the expression construct pRK5M-Tat-Flag. Twenty four hours later, the transfected cells were treated with Amt-87 (100 μ g/ml) or DMSO for 24 hr. Cells were cross-linked with 1% formaldehyde for 10 min at room temperature, which was quenched by the addition of glycine to 0.125 M for 5 min. After washing in PBS, 1 × 10⁷ cells were re-suspended in 300 μ L SDS lysis buffer (1% SDS, 10 mM EDTA, 50 mM Tris-HCl, pH 8.0) and fragmented (5 sec ON, 10 sec OFF, for a total of 20 cycles) using a Scientz JY92-IIID sonicator. The lysates were diluted 10 times with the dilution buffer (0.01% SDS, 1.1% Triton X-100, 1.2 mM EDTA, 16.7 mM Tris-HCl, pH 8.1, and 167 mM NaCl), pre-cleared with Protein A or G beads (GE), and incubated with the various antibodies (5 μ g anti-CDK9, 3 μ g anti-HEXIM1, 1.5 μ g anti-AFF4, 1.5 μ g anti-ELL2, or 2 μ g rabbit total IgG) overnight at 4 μ L. After mixing with Protein A/G beads for 1 hr, the beads were washed three times with the washing buffer (0.1% SDS, 1% Triton X-100, 2 mM EDTA, 20 mM Tris-HCl, pH 8.1, and 150 mM NaCl) and then three times with the TE buffer (10 mM Tris-HCl, pH 8.1 and 1 mM EDTA). DNA was eluted from the beads with the elution buffer (1% SDS and 100 mM NaHCO₃) and purified by phenol/chloroform extraction and ethanol precipitation. The final products were analyzed by real-time PCR with the primers listed below to amplify the integrated HIV LTR-luciferase gene. The PCR signals were normalized to the input DNA and shown as an average of three independent measurements. The sequences of the primers are:

Promoter (position 1) Forward: 5' TCCGCTGGGGACTTTCCA

Promoter (position 1) Reverse: 5' GTACAGGCAAAAAGCAGCTGC
 TAR(position 2) Forward: 5'TGCTTTTTGCCTGTACTGGGT
 TAR(position 2) Reverse: 5'CAGTACCGGAATGCCAAGCTT
 Nascent (position 3) Forward: 5' TCTGGCTAACTAGGGAACCCA
 Nascent (position 3) Reverse: 5' CGCCGGGCCTTCTTTATGT

Data Availability. All data generated or analyzed during this study are included in this published article and its Supplementary Information files.

References

1. Siliciano, J. D. & Siliciano, R. F. Recent developments in the effort to cure HIV infection: going beyond N = 1. *The Journal of clinical investigation* **126**, 409–414, doi:10.1172/JCI86047 (2016).
2. Kimata, J. T., Rice, A. P. & Wang, J. Challenges and strategies for the eradication of the HIV reservoir. *Current opinion in immunology* **42**, 65–70, doi:10.1016/j.coi.2016.05.015 (2016).
3. Deeks, S. G. Towards an HIV cure: a global scientific strategy. *Nat Rev Immunol* **12**, 607–614, doi:10.1038/Nri3262 (2012).
4. Richman, D. D. *et al.* The challenge of finding a cure for HIV infection. *Science* **323**, 1304–1307, doi:10.1126/science.1165706 (2009).
5. Jiang, G. *et al.* Reactivation of HIV latency by a newly modified Ingenol derivative via protein kinase Cdelta-NF-kappaB signaling. *AIDS*, doi:10.1097/QAD.0000000000000289 (2014).
6. Mohammadi, P. *et al.* Dynamics of HIV latency and reactivation in a primary CD4 + T cell model. *PLoS pathogens* **10**, e1004156, doi:10.1371/journal.ppat.1004156 (2014).
7. Archin, N. M. & Margolis, D. M. Emerging strategies to deplete the HIV reservoir. *Current opinion in infectious diseases* **27**, 29–35, doi:10.1097/QCO.000000000000026 (2014).
8. Cillo, A. R. & Mellors, J. W. Which therapeutic strategy will achieve a cure for HIV-1? *Current opinion in virology* **18**, 14–19, doi:10.1016/j.coviro.2016.02.001 (2016).
9. Margolis, D. M., Garcia, J. V., Hazuda, D. J. & Haynes, B. F. Latency reversal and viral clearance to cure HIV-1. *Science* **353**, aaf6517, doi:10.1126/science.aaf6517 (2016).
10. Karn, J. The molecular biology of HIV latency: breaking and restoring the Tat-dependent transcriptional circuit. *Current Opinion in HIV and Aids* **6**, 4–11, doi:10.1097/Coh.0b013e328340ffbb (2011).
11. Barton, K. M., Burch, B. D., Soriano-Sarabia, N. & Margolis, D. M. Prospects for Treatment of Latent HIV. *Clin Pharmacol Ther* **93**, 46–56, doi:10.1038/clpt.2012.202 (2013).
12. Darcis, G., Van Driessche, B. & Van Lint, C. HIV Latency: Should We Shock or Lock? *Trends in immunology* **38**, 217–228, doi:10.1016/j.it.2016.12.003 (2017).
13. Barton, K. M., Burch, B. D., Soriano-Sarabia, N. & Margolis, D. M. Prospects for treatment of latent HIV. *Clinical pharmacology and therapeutics* **93**, 46–56, doi:10.1038/clpt.2012.202 (2013).
14. Ott, M., Geyer, M. & Zhou, Q. The control of HIV transcription: keeping RNA polymerase II on track. *Cell host & microbe* **10**, 426–435, doi:10.1016/j.chom.2011.11.002 (2011).
15. He, N. *et al.* HIV-1 Tat and host AFF4 recruit two transcription elongation factors into a bifunctional complex for coordinated activation of HIV-1 transcription. *Molecular cell* **38**, 428–438, doi:10.1016/j.molcel.2010.04.013 (2010).
16. He, N. H. *et al.* HIV-1 Tat and Host AFF4 Recruit Two Transcription Elongation Factors into a Bifunctional Complex for Coordinated Activation of HIV-1 Transcription. *Molecular Cell* **38**, 428–438, doi:10.1016/j.molcel.2010.04.013 (2010).
17. Sobhian, B. *et al.* HIV-1 Tat Assembles a Multifunctional Transcription Elongation Complex and Stably Associates with the 7SK snRNP. *Molecular Cell* **38**, 439–451, doi:10.1016/j.molcel.2010.04.012 (2010).
18. Ott, M., Geyer, M. & Zhou, Q. The Control of HIV Transcription: Keeping RNA Polymerase II on Track. *Cell Host Microbe* **10**, 426–435, doi:10.1016/j.chom.2011.11.002 (2011).
19. Zhou, Q., Li, T. D. & Price, D. H. RNA Polymerase II Elongation Control. *Annu Rev Biochem* **81**, 119–143, doi:10.1146/annurev-biochem-052610-095910 (2012).
20. Zhang, Z., Klatt, A., Gilmour, D. S. & Henderson, A. J. Negative elongation factor NELF represses human immunodeficiency virus transcription by pausing the RNA polymerase II complex. *The Journal of biological chemistry* **282**, 16981–16988, doi:10.1074/jbc.M610688200 (2007).
21. Bowman, E. A. & Kelly, W. G. RNA polymerase II transcription elongation and Pol II CTD Ser2 phosphorylation: A tail of two kinases. *Nucleus* **5**, 224–236, doi:10.4161/nucl.29347 (2014).
22. Nguyen, V. T., Kiss, T. S., Michels, A. A. & Bensaude, O. 7SK small nuclear RNA binds to and inhibits the activity of CDK9/cyclin T complexes. *Nature* **414**, 322–325, doi:10.1038/35104581 (2001).
23. Yang, Z. Y., Zhu, Q. W., Luo, K. X. & Zhou, Q. The 7SK small nuclear RNA inhibits the CDK9/cyclin T1 kinase to control transcription. *Nature* **414**, 317–322, doi:10.1038/35104575 (2001).
24. Jeronimo, C. *et al.* Systematic analysis of the protein interaction network for the human transcription machinery reveals the identity of the 7SK capping enzyme. *Molecular Cell* **27**, 262–274, doi:10.1016/j.molcel.2007.06.027 (2007).
25. Krueger, B. J. *et al.* LARP7 is a stable component of the 7SK snRNP while P-TEFb, HEXIM1 and hnRNP A1 are reversibly associated. *Nucleic Acids Research* **36**, 2219–2229, doi:10.1093/Nar/Gkn061 (2008).
26. Xue, Y., Yang, Z., Chen, R. & Zhou, Q. A capping-independent function of MePCE in stabilizing 7SK snRNA and facilitating the assembly of 7SK snRNP. *Nucleic acids research* **38**, 360–369, doi:10.1093/nar/gkp977 (2010).
27. Krueger, B. J. *et al.* LARP7 is a stable component of the 7SK snRNP while P-TEFb, HEXIM1 and hnRNP A1 are reversibly associated. *Nucleic acids research* **36**, 2219–2229, doi:10.1093/nar/gkn061 (2008).
28. Cosgrove, M. S., Ding, Y., Rennie, W. A., Lane, M. J. & Hanes, S. D. The Bin3 RNA methyltransferase targets 7SK RNA to control transcription and translation. *Wiley interdisciplinary reviews. RNA* **3**, 633–647, doi:10.1002/wrna.1123 (2012).
29. Brogie, J. E. & Price, D. H. Reconstitution of a functional 7SK snRNP. *Nucleic acids research*. doi:10.1093/nar/gkx262 (2017).
30. Nowakowska, Z. A review of anti-infective and anti-inflammatory chalcones. *European journal of medicinal chemistry* **42**, 125–137, doi:10.1016/j.ejmech.2006.09.019 (2007).
31. Meng, C. Q. *et al.* Carboxylated, heteroaryl-substituted chalcones as inhibitors of vascular cell adhesion molecule-1 expression for use in chronic inflammatory diseases. *Journal of medicinal chemistry* **50**, 1304–1315, doi:10.1021/jm0614230 (2007).
32. Jung, J. C. *et al.* Efficient synthesis and neuroprotective effect of substituted 1,3-diphenyl-2-propen-1-ones. *Journal of medicinal chemistry* **51**, 4054–4058, doi:10.1021/jm800221g (2008).
33. Boumendjel, A. *et al.* Antimitotic and antiproliferative activities of chalcones: forward structure-activity relationship. *Journal of medicinal chemistry* **51**, 2307–2310, doi:10.1021/jm0708331 (2008).
34. Srinivasan, B., Johnson, T. E., Lad, R. & Xing, C. Structure-activity relationship studies of chalcone leading to 3-hydroxy-4,3',4',5'-tetramethoxychalcone and its analogues as potent nuclear factor kappaB inhibitors and their anticancer activities. *Journal of medicinal chemistry* **52**, 7228–7235, doi:10.1021/jm901278z (2009).
35. Mojzisz, J., Varinska, L., Mojziszova, G., Kostova, I. & Mirossay, L. Antiangiogenic effects of flavonoids and chalcones. *Pharmacological research* **57**, 259–265, doi:10.1016/j.phrs.2008.02.005 (2008).

36. Detsi, A., Majdalani, M., Kontogiorgis, C. A., Hadjipavlou-Litina, D. & Kefalas, P. Natural and synthetic 2'-hydroxy-chalcones and aurones: synthesis, characterization and evaluation of the antioxidant and soybean lipoxygenase inhibitory activity. *Bioorganic & medicinal chemistry* **17**, 8073–8085, doi:10.1016/j.bmc.2009.10.002 (2009).
37. Wang, C. *et al.* A Natural Product from *Polygonum cuspidatum* Sieb. Et Zucc. Promotes Tat-Dependent HIV Latency Reversal through Triggering P-TEFb's Release from 7SK snRNP. *PLoS one* **10**, e0142739, doi:10.1371/journal.pone.0142739 (2015).
38. Jordan, A., Bisgrove, D. & Verdin, E. HIV reproducibly establishes a latent infection after acute infection of T cells *in vitro*. *The EMBO journal* **22**, 1868–1877, doi:10.1093/emboj/cdg188 (2003).
39. Pearson, R. *et al.* Epigenetic silencing of human immunodeficiency virus (HIV) transcription by formation of restrictive chromatin structures at the viral long terminal repeat drives the progressive entry of HIV into latency. *Journal of virology* **82**, 12291–12303, doi:10.1128/JVI.01383-08 (2008).
40. Li, Z., Guo, J., Wu, Y. & Zhou, Q. The BET bromodomain inhibitor JQ1 activates HIV latency through antagonizing Brd4 inhibition of Tat-transactivation. *Nucleic acids research* **41**, 277–287, doi:10.1093/nar/gks976 (2013).
41. Yang, Z., Zhu, Q., Luo, K. & Zhou, Q. The 7SK small nuclear RNA inhibits the CDK9/cyclin T1 kinase to control transcription. *Nature* **414**, 317–322, doi:10.1038/35104575 (2001).
42. Williams, S. A. *et al.* Prostratin antagonizes HIV latency by activating NF- κ B. *The Journal of biological chemistry* **279**, 42008–42017, doi:10.1074/jbc.M402124200 (2004).
43. Jeronimo, C. *et al.* Systematic analysis of the protein interaction network for the human transcription machinery reveals the identity of the 7SK capping enzyme. *Molecular cell* **27**, 262–274, doi:10.1016/j.molcel.2007.06.027 (2007).
44. Chao, S. H. *et al.* Flavopiridol inhibits P-TEFb and blocks HIV-1 replication. *The Journal of biological chemistry* **275**, 28345–28348, doi:10.1074/jbc.C000446200 (2000).
45. Lu, H. *et al.* Correction: Compensatory induction of MYC expression by sustained CDK9 inhibition via a BRD4-dependent mechanism. *eLife* **4**, e09993, doi:10.7554/eLife.09993 (2015).
46. Garber, M. E. *et al.* CDK9 autophosphorylation regulates high-affinity binding of the human immunodeficiency virus type 1 tat-P-TEFb complex to TAR RNA. *Molecular and cellular biology* **20**, 6958–6969 (2000).
47. Chen, R. *et al.* PP2B and PP1 α cooperatively disrupt 7SK snRNP to release P-TEFb for transcription in response to Ca²⁺ signaling. *Genes & development* **22**, 1356–1368, doi:10.1101/gad.1636008 (2008).
48. Chen, R., Yang, Z. & Zhou, Q. Phosphorylated positive transcription elongation factor b (P-TEFb) is tagged for inhibition through association with 7SK snRNA. *The Journal of biological chemistry* **279**, 4153–4160, doi:10.1074/jbc.M310044200 (2004).
49. He, N. *et al.* A La-related protein modulates 7SK snRNP integrity to suppress P-TEFb-dependent transcriptional elongation and tumorigenesis. *Molecular cell* **29**, 588–599, doi:10.1016/j.molcel.2008.01.003 (2008).
50. Nguyen, V. T., Kiss, T., Michels, A. A. & Bensaude, O. 7SK small nuclear RNA binds to and inhibits the activity of CDK9/cyclin T complexes. *Nature* **414**, 322–325, doi:10.1038/35104581 (2001).
51. Yik, J. H. *et al.* Inhibition of P-TEFb (CDK9/Cyclin T) kinase and RNA polymerase II transcription by the coordinated actions of HEXIM1 and 7SK snRNA. *Molecular cell* **12**, 971–982 (2003).
52. Laroche, S. & Fisher, R. P. CDK-activating kinases: detection and activity measurements. *Methods in molecular biology* **296**, 279–290 (2005).
53. Yang, Z. Y. *et al.* Recruitment of P-TEFb for stimulation of transcriptional elongation by the bromodomain protein brd4. *Molecular Cell* **19**, 535–545, doi:10.1016/j.molcel.2005.06.029 (2005).
54. Li, Z. C., Guo, J., Wu, Y. T. & Zhou, Q. The BET bromodomain inhibitor JQ1 activates HIV latency through antagonizing Brd4 inhibition of Tat-transactivation. *Nucleic Acids Research* **41**, 277–287, doi:10.1093/Nar/Gks976 (2013).
55. Lu, H. *et al.* AFF1 is a ubiquitous P-TEFb partner to enable Tat extraction of P-TEFb from 7SK snRNP and formation of SECs for HIV transactivation. *Proceedings of the National Academy of Sciences of the United States of America* **111**, E15–24, doi:10.1073/pnas.1318503111 (2014).

Acknowledgements

This work is supported by grants from the National Natural Science Foundation of China (81672955), the Fundamental Research Funds for the Central Universities (20720160062), and the Natural Science Foundation of Fujian Province (2016J01172) to Y.X. It is also supported by Public Health Service grant R01AI041757 from the National Institutes of Health, USA to Q.Z.

Author Contributions

Y.-h.X. conceived the project, analyzed the data, wrote the paper. Q.Z. conceived the project, analyzed the data, wrote the paper. Z.W. conceived the project, analyzed the data, wrote the paper. J.W. performed the experiments. M.A. performed the experiments. R.S. performed the experiments. H.W. performed the experiments. D.Y. performed the experiments. M.F. analyzed the data. X.G. analyzed the data. All authors reviewed the manuscript.

Additional Information

Supplementary information accompanies this paper at doi:10.1038/s41598-017-10728-w

Competing Interests: The authors declare that they have no competing interests.

Publisher's note: Springer Nature remains neutral with regard to jurisdictional claims in published maps and institutional affiliations.



Open Access This article is licensed under a Creative Commons Attribution 4.0 International License, which permits use, sharing, adaptation, distribution and reproduction in any medium or format, as long as you give appropriate credit to the original author(s) and the source, provide a link to the Creative Commons license, and indicate if changes were made. The images or other third party material in this article are included in the article's Creative Commons license, unless indicated otherwise in a credit line to the material. If material is not included in the article's Creative Commons license and your intended use is not permitted by statutory regulation or exceeds the permitted use, you will need to obtain permission directly from the copyright holder. To view a copy of this license, visit <http://creativecommons.org/licenses/by/4.0/>.

© The Author(s) 2017